Journal of Engg. Research Vol. 7 No. (1) March 2019 pp. 1-16

Uncertainty analysis for hydraulic cylinder pressure calculation of orienter in coiled tubing drilling

Meng Li*, Kanhua Su*, Lifu Wan*, Jilin Liu*, Chengwei Qi* and Weiqing Chen**

** School of Petroleum Engineering, Chongqing University of Science and Technology, Chongqing, 401331, China*
*** College of Petroleum Engineering & Geosciences, KFUPM, 31261, Saudi Arabia*
**Corresponding Author: sukanhua1978@163.com (Kanhua Su), wanlifucup@163.com(Lifu Wan)*

ABSTRACT

Orienter working pressure for coiled tubing drilling (CTD) is associated with the randomness of torque. Thus, a new method for orienter pressure design was built based on uncertainty analysis theory. The Monte-Carlo method was applied to simulate the distribution of torque parameters. The distribution types and functions of torque were obtained. Based on the functional relationship between the hydraulic cylinder working pressure and the friction torque, the probability distribution of working pressure was obtained with the probability theory. The control variable method was adopted to analyze the range of the hydraulic cylinder working pressure. Results show that working pressure is not a single value but an interval with cumulative probability change. The higher the confidence level, the narrower the pressure range, conversely, the wider the pressure range. The larger the mean square deviation, the wider the pressure range. With this new method, working pressure range of the orienter is obtained from 3.93 to 11.71 MPa, Uncertainty analysis method can overcome the disadvantages of traditional method and provide more accurate references for hydraulic cylinder design of orienter in CTD.

Keywords: torque; working pressure; uncertainty; Monte-Carlo; CTD.

INTRODUCTION

In recent years, coiled tubing drilling (CTD) technology has been greatly improved with continuous innovation and continuous improvement of the equipment and downhole tools for CTD. CTD is suitable for old well drilling deeper, slimhole drilling, directional well drilling, and sidetrack drilling. However, as the coiled tubing (CT) is not rotatable, it is necessary to use the orienter to adjust the tool face to control the trajectory of the well (Liu et al., 2011; Li et al., 2015).

Therefore, the orienter is the core tool for the trajectory control of CTD. The orienter consists of two types, mechanical orienter and electro-hydraulic driven orienter (EHO), and the latter is the most widely used; it is because the directional precision of the latter is higher and the output torque is higher (Li et al., 2015). To adjust the tool face, the Electro-hydraulic orienter should overcome the friction torque between the downhole tool and the well wall through the work of the hydraulic cylinder. Thus, the precondition of controlling trajectory for CTD is that the orienter must overcome the downhole friction torque. The scholars have done some research on the friction torque of the downhole pipe. Gao et al. (2003) carried out the force analysis of the pipe column unit for the 3D well and established a general model and algorithm for calculating the downhole friction torque. Based on the three-moment equation, the method of numerical iteration is used to establish the model of solving the friction torque at each point of the pipe column (Ciccola 2007). The influence of viscous force, inertia force, and static shear force on the force of pipe column are considered, and the friction torque model of the downhole pipe column is established (Samuel et al., 2009). Liu (2017) analyzed the friction torque of each section of the pipe under the positive rotation and reversal working conditions, and then established the basic calculation equation of the frictional force model of the downhole whole pipe. However, the randomness of the model parameters is not taken into account in all these models.

In fact, the downhole environment is complex during CTD. There are various factors affecting the friction torque, like weight on bit, mud property, tool structure, formation friction factor, etc., and all these factors have some randomness. The structures and performance parameters of the pipes are measured and the distribution states

of these parameters are obtained (Adams et al., 1993). Cunha et al. (2005) carried out a lot of experiments on weight on bit and fluid parameters during drilling, and found that all the parameters were in the form of some certain distributions. Deo et al. (2009) obtained the probability distribution of the parameters of the underground rock mechanics by using the probability statistics. Li et al. (2017) pointed out that, due to the complexity of oil and gas geology and the accuracy deviation of mathematical models, the true value of frictional torque model parameters can not be obtained, and its error exists objectively, and the parameters of the obtained model have different degrees of dispersion or uncertainty.

Because of the uncertainty of the parameters affecting the friction torque in CTD, the uncertainty of friction torque is unavoidable. According to the principle of uncertainty propagation (Goldsworthy et al., 2007), there are some uncertainties in the designed working pressure of the hydraulic cylinder obtained from the friction torque. Many scholars have done some similar studies. Maeda et al. (2003) considered the uncertainty of the load and used the Latin hypercube sampling to simulate the distribution probability of the key parameters of the working pressure of the hydraulic cylinder of the crane. Yoon et al. (2009) considered the uncertainty of the load and material performance of the component; the safety factor of the working pressure of the hydraulic cylinder of the excavator is corrected. Considering the three uncertain variables of lifting dynamic load coefficient, wire rope deflection angle, and plate thickness, a probabilistic and non-probabilistic mixed uncertainty design method is proposed, and the uncertainty of crane hydraulic cylinder working pressure is designed (Edwards et al., 2010). But at present, there is no special uncertainty design for the working pressure of the hydraulic cylinder of the CTD orienter.

Therefore, in this study, based on the uncertainty theory, the working pressure of the hydraulic cylinder is designed and calculated by using the Monte-Carlo method. The aim is to make up for the shortcomings of the traditional single value design method. The traditional single value design method may cause the lower design working pressure of the hydraulic cylinder, which would cause the orienter not to move the tool face. Traditional single value design method may also cause higher design working pressure of hydraulic cylinder, which would require higher requirements for hydraulic cylinder design, including sealing design, and may cause unnecessary waste. The uncertainty design method will provide a more reliable theoretical basis for the design of the hydraulic cylinder of the CTD orienter.

TORQUE DISTRIBUTION

1.1 TORQUE PREDICTION MODEL

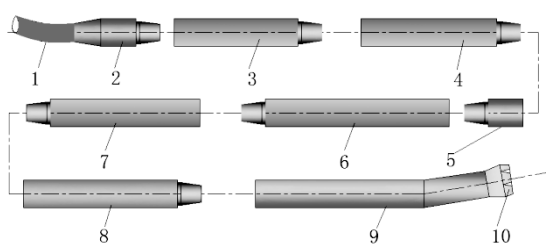

1-Coiled tubing 2-Connector 3-Power and Communication sub 4-Electrical Disconnect and Circulating Sub 5 - Connector 6 - Drilling performance sub 7 - MWD 8 - EHO 9 - Mud motor 10 - Bit

Figure 1. Configuration of BHA for CTD.

Assumptions of the model:

(1) Bend motor is simplified to the equivalent drill collar.

(2) The wall of well is stiff; the contact way between elbow point of bend motor and wall of well is point contact.

(3) Bit center is on the center line of the borehole.

(4) The vibration of BHA (bottom hole assembly) is ignored.

Model Foundation:

The BHA of CTD is shown in Fig. 1. The end of EHO is the output shaft. The end of the output shaft connects the motor with thread. There are n contact points between the borehole wall and BHA of CTD. Thus, BHA is divided into n+1 vertical and horizontal bend beams. To determine the contact points number under the output shaft of EHO, the location of the 1st upper tangent point in 3D well should be determined. The force analysis of bending motor-BHA is shown in Fig. 2. Note that plane *P* is inclination plane; plane *Q* is azimuth plane.

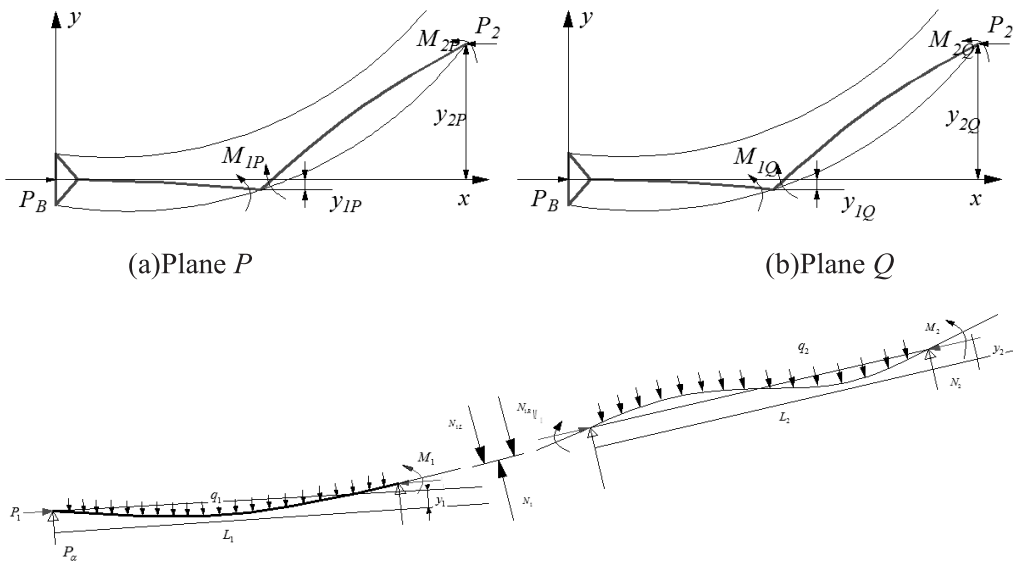

(a)Plane *P* (b)Plane *Q*

(c) Force analysis

Figure 2. Force analysis of bending motor-BHA.

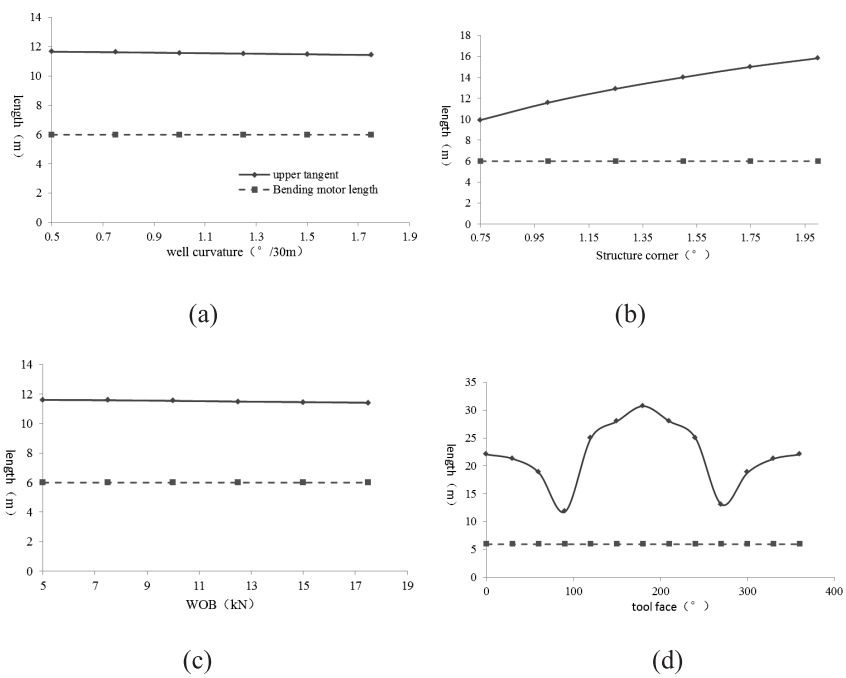

(a) (b)

(c) (d)

Figure 3. The location of the 1st upper tangent point.

Based on three-moment equation of BHA (Su et al., 1991), the location of the 1st upper tangent point was obtained by using dichotomy and numerical iteration method, shown in Fig. 3. Generally, the length of bend motor used in CTD is less than 6 m (Guan et al., 2005). Thus, the location of the 1st upper tangent point is upper than the location of the output shaft of EHO. Therefore, there is only one contact point below the EHO (in addition to the point of the bit), and the point is the elbow of bend motor.

Thus, based on continuous beam-column theory (Pessier et al., 1992; Eric et al., 2004), three-moment equation of bend motor and EHO in planes P and Q was established:

$$\begin{cases} 2M_1\left[Y(u_1)+\dfrac{L_2I_1}{L_1I_2}Y(u_2)\right]+M_2\left[\dfrac{L_2I_1}{L_1I_2}Z(u_2)\right] \\ =-\dfrac{q_1L_1^2}{4}X(u_1)-\dfrac{q_2L_2^2}{4}\cdot\dfrac{L_2I_1}{L_1I_2}X(u_2)-\dfrac{6EI_1}{L_1}\left(\dfrac{y_1}{L_1}-\dfrac{y_2-y_1}{L_2}+\gamma\right) \\ q_2X(u_2)L_2^4+4\left[2M_2Y(u_2)+M_1Z(u_2)\right]L_2^2 \\ =24EI_2\left[L_2(L_1+L_2)K-y_2+y_1\right] \end{cases} \tag{1}$$

Note that $q_1 = q_2 = 0$ in plane Q.

The reaction force at the elbow is

$$\begin{aligned} N_{1P} &= \frac{P_B y_{1P} - M_{1P}}{L_{1P}} + \frac{M_{2P} - M_{1P} + P_{1P}(y_{2P} - y_{1P})}{L_{2P}} + \frac{q_{1P}L_{1P} + q_{2P}L_{2P}}{2} \\ N_{1Q} &= \frac{P_B y_{1Q} - M_{1Q}}{L_{1Q}} + \frac{M_{2Q} - M_{1Q} + P_{1Q}(y_{2Q} - y_{1Q})}{L_{2Q}} + \frac{q_{1Q}L_{1Q} + q_{2Q}L_{2Q}}{2} \end{aligned} \tag{2}$$

$$N_1 = \sqrt{N_{1P}^2 + N_{1Q}^2} \tag{3}$$

Therefore, the total torque for adjusting the tool face is

$$T = \left|\mu_F N_1 \frac{D_0}{2} \pm \frac{1}{3}\mu P_B D_0\right| \tag{4}$$

Note that '+' represents the output shaft rotation and bit rotation is in the opposite direction; '−' represents the rotation is in the same direction.

1.2 THE TORQUE DISTRIBUTION ANALYSIS WITH MONTE-CARLO METHOD

The torque model between the downhole tool and borehole wall is a function of multiple parameters. There is some randomness for each parameter and the randomness follows a certain distribution (Long et al., 2013; Liu et al., 2010; Di et al., 2003). A large number of statistical tests (Blount et al., 1998; Leising et al., 1996) indicate that most of the parameters follow a normal distribution, such as mud density, weight on bit. Some parameters follow a lognormal distribution, like friction factor in the well. Some parameters follow a uniform distribution, like borehole curvature.

The randomness of the parameters determines the uncertainty of the torque. Based on the formula method, a state function of torque model is established.

$$T = g(\mu_F, \rho_m, K, E, P_B, D_o, \ ) \tag{5}$$

where P_m is mud density, g/cm^3; K is borehole curvature, °/30m.

Assuming the probability density function of each parameter is $f_i(x_i)$, the corresponding cumulative probability

function is $F_i(x_i)$. All parameters are made from random sampling tests with Monte-Carlo method (De et al., 2006; O'Coonor et al., 2000). After n=10000 times of simulation, the statistical distribution results of parameters are obtained, shown in Fig. 4 (a) ~ Fig. 4 (e), and the n order state matrix of parameters is

$$\mathbf{X} = \left(\boldsymbol{x}_1, \boldsymbol{x}_2, \quad , \boldsymbol{x}_m\right)^{\mathrm{T}} = \begin{pmatrix} x_{11} & x_{12} & x_{1n} \\ x_{21} & x_{22} & x_{2n} \\ & & \\ x_{m1} & x_{m2} & x_{mn} \end{pmatrix} \tag{6}$$

By applying the n order state matrix of parameters into the torque state function $T = g\left(\boldsymbol{x}_1, \boldsymbol{x}_2, \quad , \boldsymbol{x}_m\right)$, and the result is

$$\begin{pmatrix} T_1 \\ T_2 \\ \\ T_n \end{pmatrix} = \begin{pmatrix} g\left(x_{11}, x_{21}, \quad , x_{m1}\right) \\ g\left(x_{12}, x_{22}, \quad , x_{m2}\right) \\ \\ g\left(x_{1n}, x_{2n}, \quad , x_{mn}\right) \end{pmatrix} \tag{7}$$

The mean value of friction torque is $\mu_T = \frac{1}{n}\sum_{i=1}^{n} T_i$, and the standard deviation is $\sigma_T = \sqrt{\frac{1}{n-1}\sum_{i-1}^{m}\left(T_i - \mu_T\right)}$. Through the numerical fitting, the torque distribution curve is got, shown in Fig. 4, where x_1 are the parameters of torque, i =1,2,3, m; x_{ij} is the random value ofafter simulation, j =1,2,3, n.

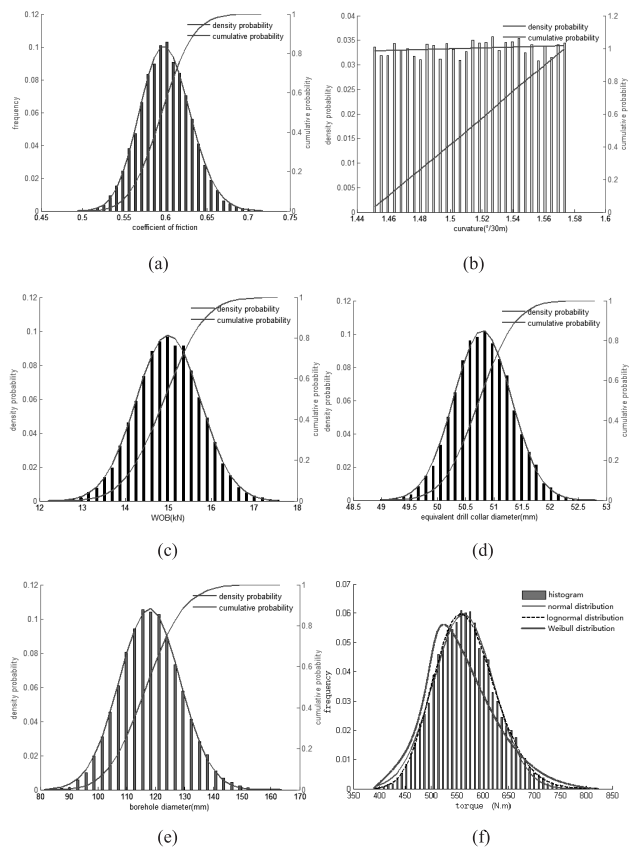

Figure 4. Distribution types of friction torque.

Fig. 4 (f) illustrates that normal and lognormal distribution fitting curves are more consistent with histogram distribution law of torque than Weibull distribution curve. The corresponding probability density functions are (Wonneberger et al.,1994; Sun et al., 2003):

Normal distribution:

$$h(T)=\frac{A}{\sigma\sqrt{\pi/2}}e^{-2\frac{(T-\mu)^2}{\sigma^2}} \tag{8}$$

where $[A,\mu,\sigma]=[9.18,562.36,118.78]$.

Lognormal distribution:

$$h(T)=\frac{A}{\sigma\sqrt{2\pi}T}e^{-\frac{(\ln T-\mu)^2}{2\sigma^2}} \tag{9}$$

where $[A,\mu,\sigma]=[9.21,6.33,0.11]$.

After correlation tests for fitting function and the frequency distribution of torque, the normal and lognormal standard deviations are 60.04 and 54.83, respectively. The results indicate that lognormal distribution for the uncertainty of the torque is more accurate. Parameters distribution and the torque distribution are given in Table 1.

Table 1. Distribution types of torque and parameters.

parameters	distribution type	reference		parameters	distribution type	reference	
		μ	σ			μ	σ
friction coefficient	Log-normal ln-N(μ, σ^2)	0.55	0.08	wellbore diameter	normal N(μ, σ^2)	118	5.9
bit weight	normal N(μ, σ^2)	15002	746.8	equivalent collar external diameter	normal N(μ, σ^2)	104.8	1.0
mud density	normal N(μ, σ^2)	1.1	0.01	Equivalent collar inner diameter	normal N(μ, σ^2)	88.9	0.8
steel density	normal N(μ, σ^2)	7.8	0.008	the location of the upper tangent point	normal N(μ, σ^2)	11.5	0.23
tool length below elbow	normal N(μ, σ^2)	1.5	0.015	bend angle	normal N(μ, σ^2)	1.5	0.015
curvature	uniform U(a,b)	1.45	1.55	elastic modulus of BHA	normal N(μ, σ^2)	209	2

1.3 THE EFFECT OF PARAMETERS' VARIATION ON THE UNCERTAINTY OF TORQUE

In engineering application, the effect of different parameters on the uncertainty of torque is different. The variation coefficients are the indicators of uncertainty. Thus, this article analyzes the influence of the variation coefficients of parameters on the variation coefficient of torque. The variation coefficient is defined as follows (De et al., 2006):

$$COV = \frac{Mean}{Standard\ \ deviation} \tag{10}$$

where COV is variation coefficient.

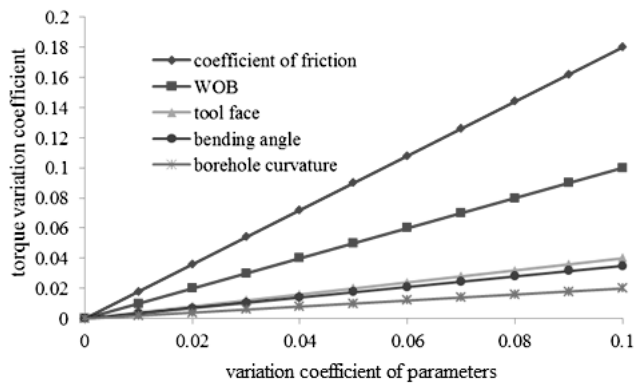

Fig5. The effect of parameters randomness on the torque uncertainty

As Fig. 5 shows, the uncertainty of the torque increases linearly with the variation coefficient of parameters varying from 0 to 0.1. Among these parameters, the randomness of formation friction factor and weight on bit imposes a greater influence on the uncertainty of the torque, whereas the randomness of the other parameters, such as tool-face angle, well curvature, plays a smaller influence on the uncertainty of friction torque.

THE WORKING PRESSURE DISTRIBUTION OF ORIENTER HYDRAULIC CYLINDER

2.1 THE HYDRAULIC CYLINDER PRESSURE MODEL

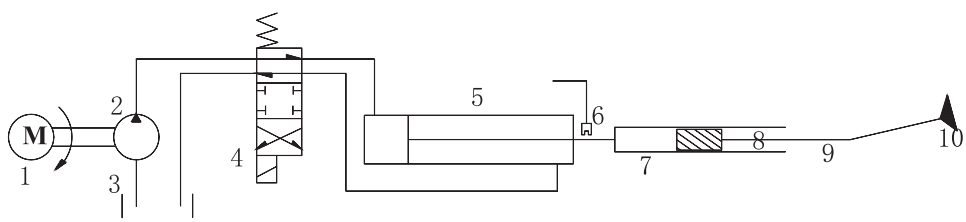

1- micro electric motor 2-miniature hydraulic pump 3 - sealed tank 4 - electromagnetic directional valve 5 - hydraulic cylinder 6 - displacement sensor 7 - sliding nut 8 - screw mandrel 9 - bend motor 10 - bit

Figure 6. Working principle of EHO orienter.

As shown in Fig. 6, the working principle of the electro-hydraulic orienter is as follows: The micro electric motor drives miniature hydraulic pump operation, then the hydraulic oil is pumped into the hydraulic cylinder through the electromagnetic directional valve. The motion of the piston in the cylinder will promote sliding nut and screw mandrel interaction with each other, then tool face of bend motor is rotated. Thus, orientation while drilling will be achieved. The interaction force analysis between the sliding nut and screw mandrel is shown in Fig. 7.

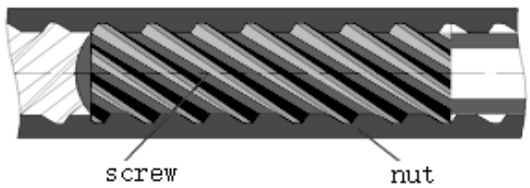

(a) The structure of sliding nut and screw mandrel

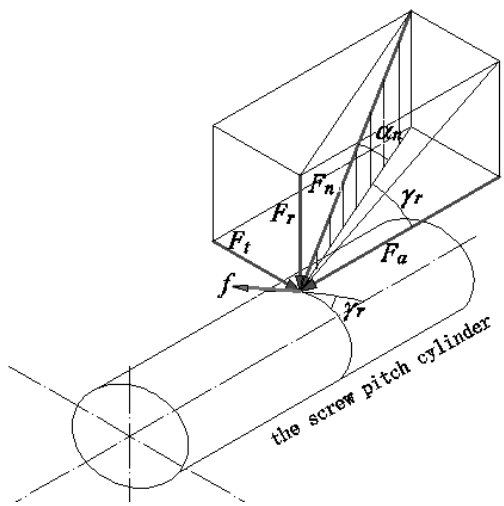

(b) force analysis

Figure 7. Force analysis of screw mandrel.

The structures of sliding nut and screw mandrel are shown in Fig. 7 (a). To simplify the calculation process, the screw reference cylinder is chosen for force analysis. A concentrated force replaces all the distributed force on the splines. As shown in Fig.7 (b), the force component of F_n is axial force F_a , tangent force F_t, radial force F_r (units are N). Due to the screw, axial is center-symmetric, and radial force F_r can be offset with each other.

According to the force analysis in Fig. 7, the following equations are listed.

$$\begin{cases} R = F_a + f \cdot \sin\gamma_r \\ F_t = F_a \tan\gamma_r \\ F_t - f\cos\gamma_r = \dfrac{2T}{d} \\ f = \mu_r F_n \\ F_n = \dfrac{F_t}{\sin\gamma_r \cos\alpha_n} \\ F_a = \dfrac{2T}{\left(\tan\gamma_r - \dfrac{\mu_r}{\cos\alpha_n}\right)d} \end{cases} \tag{11}$$

Hence, the axial thrust is

$$R = \frac{2T\left(\cos\alpha_n + \mu_r \tan\gamma_r\right)}{\left(\tan\gamma_r \cdot \cos\alpha_n - \mu\right)d} \tag{12}$$

$$\text{Also,} \quad p\Delta A\eta = R \tag{13}$$

Therefore, the working pressure of hydraulic cylinder is

$$p = \frac{2T\left(\cos\alpha_n + \mu_r \tan\gamma_r\right)}{\eta\left(\tan\gamma_r \cdot \cos\alpha_n - \mu_r\right)d\Delta A} \tag{14}$$

where $\Delta A = \begin{cases} A_1 & \textit{The piston out} \\ A_1 - A_2 & \textit{The piston in} \end{cases}$

Equation (4) is brought into the equation (14) to obtain the equation (15):

$$p = \begin{cases} \dfrac{2\mu\left(\cos\alpha_n + \mu_r \tan\gamma_r\right)}{\eta\left(\tan\gamma_r \cdot \cos\alpha_n - \mu_r\right)A_1 d}\left(N_1 \dfrac{D_0}{2} + \dfrac{1}{3} \cdot WOB \cdot D_0\right) & \textit{The piston out} \\ \dfrac{2\mu\left(\cos\alpha_n + \mu_r \tan\gamma_r\right)}{\eta\left(\tan\gamma_r \cdot \cos\alpha_n - \mu_r\right)\left(A_1 - A_2\right)d}\left(\dfrac{1}{3} \cdot WOB \cdot D_0 - N_1 \dfrac{D_0}{2}\right) & \textit{The piston in} \end{cases} \tag{15}$$

where R is the workload of the hydraulic cylinder, and N; μ_r is the friction factor between the sliding nut and screw; here, it is 0.1; d is the diameter of screw, mm; p is working pressure of hydraulic cylinder, Pa; ΔA is the effective working area of piston, mm^2; η is mechanical efficiency; here, it is 0.95.

2.2 Working pressure distribution form of hydraulic cylinder

Using t as the random value of the friction torque T, using Y instead of working pressure p, y as the random value of Y, thus, equation (14) can substitute equation (16):

$$y = s(t) = \frac{2t\left(\cos\alpha_n + \mu_r \tan\gamma_r\right)}{\eta\left(\tan\gamma_r \cdot \cos\alpha_n - \mu_r\right)d\Delta A} \tag{16}$$

$$t = s^{-1}(t) = k(y) = \frac{\left(\tan\gamma_r \cdot \cos\alpha_n - \mu_r\right)d\Delta A\eta}{2\left(\cos\alpha_n + \mu_r \tan\gamma_r\right)}y \tag{17}$$

The derivation of the equation $k(y)$ is

$$k'(y) = \frac{\left(\tan\gamma_r \cdot \cos\alpha_n - \mu_r\right)d\Delta A\eta}{2\left(\cos\alpha_n + \mu_r \tan\gamma_r\right)} \tag{18}$$

With the distribution of the torque, the distribution function of working pressure can be obtained based on equation (19) (Sun, et al., 2003):

$$p_Y(y) = p_T\left(k(y)\right)\left|k'(y)\right| \tag{19}$$

As illustrated in section 1.2, the uncertainty distribution of torque is lognormal distribution. Hence, the distribution of the working pressure can be derived from equation (19).

The probability density function of the working pressure is

$$p_Y(y) = \frac{2}{\sqrt{2\pi}\sigma}\frac{\left(\cos\alpha_n + \mu_r \tan\gamma_r\right)}{\left(\tan\gamma_r \cdot \cos\alpha_n - \mu_r\right)d\Delta A\eta} \times \exp\left[-\frac{\left\{\ln\left[\dfrac{\left(\tan\gamma_r \cdot \cos\alpha_n - \mu_r\right)d\Delta A\eta}{2\left(\cos\alpha_n + \mu_r \tan\gamma_r\right)}y\right] - \mu\right\}^2}{2\sigma^2}\right] \tag{20}$$

The cumulative probability distribution function is

$$F_Y(y)=\frac{1}{\sqrt{2\pi}\sigma}\int_0^{\frac{(\tan\gamma_r\cdot\cos\alpha_n-\mu_r)d\Delta\eta}{2(\cos\alpha_n+\mu_r\tan\gamma_r)}y}\frac{1}{t}\exp\left[-\frac{(t-\mu)^2}{2\sigma^2}\right]dt \tag{21}$$

Probability density distribution and cumulative probability distribution curves of working pressure are given in Fig. 8.

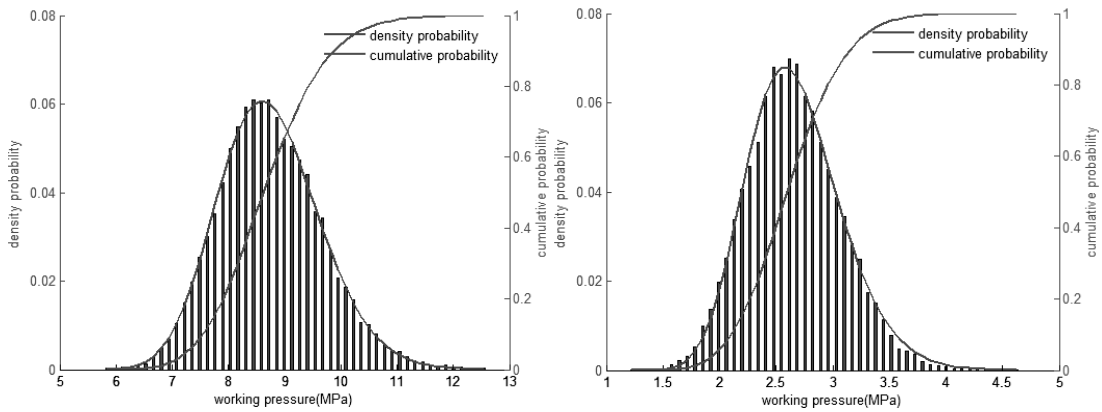

（a）the piston out （b）the piston in

Figure 8. Distribution of working pressure.

As shown in Fig. 8, during orientation for CTD, working pressure is larger in the piston out process than in the piston retraction process. Therefore, working pressure in the piston out process is taken as the research object for the hydraulic cylinder design.

CASE STUDY

At present, most of the wells for CTD are shallow wells. Because the coiled tubing is a flexible tube, it is difficult to apply weight on bit during CTD. The weight on bit is generally less than 15 kN. According to the paper (Blount et al., 1998), the friction coefficient between BHA and borehole wall is generally between 0.4 and 0.65. The other parameters for calculating working pressure during CTD are as follows: the outside diameter and equivalent inner diameter of bend motor are 104.8 mm and 88.9 mm, respectively; the structure corner is 1.5°, the well curvature is 1.5°/30m, the mud density is 1.1 g/cm^3, normal pressure angle of spline is 20°, lead angle of spline is 75°, mechanical efficiency of hydraulic cylinder is 0.95, piston diameter is 40.6 mm, and the piston rod diameter is 17 mm. Based on the uncertainty calculation method in this paper, working pressure of orienter's hydraulic cylinder during CTD is analyzed. The working pressure curves for the cumulative probability of 5% and 95% with parameters variation are illustrated in Fig. 9. For a designer, the potential range of HC working pressure is more effective and actual than a single pressure value. With the pressure range, the designer will provide a more accurate design program for HC lifetime prediction, HC seal design, and the selection of miniature hydraulic pump.

Based on the probability theory, the equation for a confidence interval of working pressure is (Sun et al., 2003)

$$f_p\left(\sigma_p,u_{1-\frac{\alpha}{2}}\right)=\left[\overline{P}-\frac{\sigma_p}{\sqrt{n}}u_{1-\frac{\alpha}{2}},\ \ \overline{P}+\frac{\sigma_p}{\sqrt{n}}u_{1-\frac{\alpha}{2}}\right] \tag{22}$$

The derivation of equation (22) is

$$\begin{cases} \dfrac{\partial f_p}{\partial \sigma_P} = \left[-\dfrac{1}{\sqrt{n}} u_{1-\frac{\alpha}{2}}, \dfrac{1}{\sqrt{n}} u_{1-\frac{\alpha}{2}} \right] \\ \dfrac{\partial f_p}{\partial u_{1-\frac{\alpha}{2}}} = \left[-\dfrac{\sigma_P}{\sqrt{n}}, \dfrac{\sigma_P}{\sqrt{n}} \right] \end{cases} \tag{23}$$

Note that $\overline{P}$ is sample estimation of the mean pressure, MPa; σ_p is the standard deviation of the mean pressure, MPa; $u_{1-\frac{\alpha}{2}}$ is quantile of confidence level , $1-\dfrac{\alpha}{2}$, $0<$.

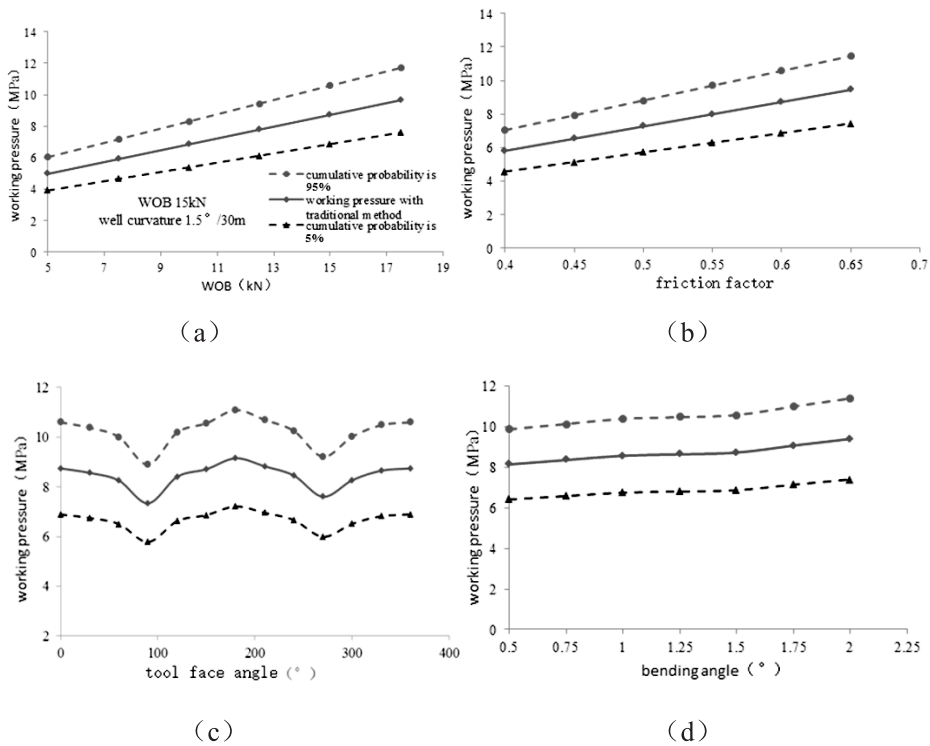

Figure 9. Working pressure curves of hydraulic cylinder during orientation.

Fig. 9 illustrates the difference between the uncertainty method and the traditional method. The working pressure based on the uncertainty method is not a single value but a pressure interval. As the pressure increases, the pressure interval becomes wider. It is because the mean square deviation of working pressure increases with the working pressure increasing.

Equation (23) illustrates that the higher the confidence level, the greater the pressure interval. Conversely, the lower the confidence level, the smaller the pressure interval. Hence, the size of the pressure range is related to the accuracy of the parameters. Thus, more accurate parameters are usually required. However, it is generally difficult to obtain sufficiently accurate information for the complexity of downhole conditions. Therefore, it is necessary to design HC working pressure by using the uncertainty analysis method.

In order to get the HC working pressure range, the working pressure intervals with parameters' variation during CTD are obtained by using control variable method. According to equation (15), the traditional single value calculation method, the traditional working pressure intervals A are obtained (Table 2). According to equations (21) and (22), the uncertainty calculation method, the working pressure intervals B between the cumulative probability are 5% (the lower limit of working pressure) and 95% (the upper limit of working pressure) (Table 2).

Table 2. The hydraulic cylinder working pressure range of orienter.

main parameters	parameter intervals	pressure intervals A(MPa)	pressure intervals B(MPa)
WOB (kN)	[5.0,17.5]	[5.00,9.66]	[4.23,11.71]
Friction coefficient	[0.4,0.65]	[5.81,9.46]	[4.58,11.46]
Tool face (°)	[0,360]	[7.34,9.15]	[5.78,11.09]
Bend angle (°)	[0.5,2.25]	[8.15,9.40]	[6.41,11.41]
Well curvature (°/30m)	[0.5,2.0]	[8.65,8.88]	[6.81,10.77]
Mud density (g/cm^3)	[1.0,1.8]	[8.69,8.72]	[6.93,10.65]

According to equation (24), the working pressure range of HC during CTD is obtained:

$$\begin{cases} p_{\max} = \max\left\{p_{i\max}\right\} & i = 1,2,3,\ldots,m \\ p_{\min} = \min\left\{p_{i\min}\right\} & i = 1,2,3,\ldots,m \end{cases} \tag{24}$$

As shown in Table 2 and equation (24), the working pressure range obtained with the uncertainty analysis method is [4.23, 11.71] MPa, and the range obtained with the traditional calculation method is [5.00, 9.66] MPa. The randomness of the parameters can enlarge the working pressure range, but the traditional method considers the parameters as fixed values. Therefore, the pressure range obtained from the latter is limited. The uncertainty design method can provide a more accurate theoretical guidance for HC lifetime prediction, seal design, and the selection of miniature hydraulic pump.

CONCLUSIONS

(1) Based on continuous beam-column theory, the torque model between BHA and well wall during tool face rotation in CTD under the condition of the 3D well is established.

(2) The parameters of the torque are random, and each parameter follows a certain distribution function. Thus, the distributed simulation of the parameters is carried out by using Monte-Carlo method, and the result shows that the distribution of torque is lognormal.

(3) The function for the pressure of HC and torque is established. The distribution of working pressure is lognormal deduced from probability theory.

(4) Due to the randomness of the parameters, there are some limitations for the traditional fixed value calculation method. The working pressure range of HC obtained through the uncertainty analysis method is closer to the practical working pressure value in CTD. The uncertainty analysis method can provide more accurate references for HC design of orienter in CTD.

Nomenclature

BHA : bottom hole assembly.
COV : variation coefficient.
CT : coiled tubing.
CTD : coiled tubing drilling.
EHO : electro-hydraulic driven orienter.
HC : hydraulic cylinder.
WOB : weight on bit.

d : the diameter of screw, mm.

D_o : wellbore diameter, mm.

E : elastic modulus of BHA, Pa.

f : the friction force between the sliding nut and screw, N.

F_a : axial force, N.

F_t : tangent force, N.

F_r : radial force, N.

I_i is : inertia moment of the i^{st} BHA, cm^4

K : borehole curvature, °/30m.

L_i : the length of the i^{st} BHA, m.

M_i : the bending moment at the i^{st} contact point, N.m.

N_1 : is reaction force, N.

N_{1P}, N_{1Q} : reaction force in plane *P, Q*.

P : working pressure of hydraulic cylinder, Pa.

P_{max}, P_{min} : the maximum and minimum values of the working pressure, MPa.

$P_{i\,max}$, $P_{i\,min}$: the maximum value, the minimum value of working pressure with the influence of the i^{st} parameter, MPa.

P_B : bit weight, N.

$\overline{P}$: sample estimation of the mean pressure, MPa.

q_i : the uniformly distributed load on the lateral of the i^{st} BHA, N/m.

R : the workload of the hydraulic cylinder, N. $u_{1-\frac{\alpha}{2}}$: quantile of confidence level $1-\frac{\alpha}{2}$, $0<\alpha<1$.

w_i : the buoyant weight of the ist BHA in the mud, N/m.

y_{1P}, y_{1Q} : *y*-coordinate values of elbow in plane *P, Q,* m.

y_{2P}, y_{2Q} : y-coordinate values of upper tangent point in plane P, Q, m.

$X(u_i)$, $Y(u_i)$, $Z(u_i)$: the deformation ratios, the solving processes refer to the paper (Su et al., 1991). a_i: the average deviation angle of the ist i^{st} BHA, °.

a_n : pressure angle, °.

r : the bend angle of motor, °.

γ_r : the lead angle, °.

ΔA : the effective working area of piston, mm^2.

η : mechanical efficiency, here is 0.95.

μ : friction factor between BHA and wellbore.

μ_F : is friction factor between BHA and wellbore.

μ_r : the friction factor between the sliding nut and screw, here is 0.1.

ρ_m : mud density, g/cm^3.

σ_p : the standard deviation of the mean pressure, MPa.

ACKNOWLEDGMENT

This work was supported by the National Natural Science Foundation of China [51804061], [51774063], the Academician Led Special Project of Chongqing Science and Technology Commission [CSTC2017zdcy-yszxX0009], and the Chongqing Research Program of Basic Research and Frontier Technology [CSTC2018jcyjA1459].

REFERENCES

Liu, Q. Y., Qu, D. & Li, W. 2011. The application of unconventional gas development in China for CTD. China Petroleum Machinery, (39):94–100

Li, M., He, H. Q. & Zhang. Y. F. 2015. The status and development suggestion on the coiled tubing drilling orienter. China Petroleum Machinery, **43**(1): 32–38

Gao, D. L. & Jin, T. J. 2003. Research on numerical analysis of drag and torque for xijiang extended reach wells in south-china sea. Oil Drilling &Production Technology, **25**(5):89–93.

Ciccola, V. L. 2007. Casing and liner drag forces as design and analysis parameter for complex architecture wells. SPE 107185.

Samuel, G. R. & Mason, C. J. 2009. Surge and drag analysis for extended reach casing and casing flotation operations with centralizers. SPE Drilling & Completion; **24**(4):473–483.

Liu, Z. H. 2016. Research on the mechanical properties of rotary drill tool. Yangtze University, 56–60.

Adams, A. J., Parfitt, S. H. L., Reeves, T. B. & Thorogood, J. L. 1993. Casing system risk analysis using structural reliability. SPE/IADC 25693.

Cunha, J. C., Demirdal, B. & Gui, P. 2005. Use of quantitative risk analysis for uncertainty quantification on drilling operations review and lessons learned. SPE 94980.

Deo, P., Xue, C. & Mendez, F. 2009. Managing uncertainty of well log data in reservoir characterization. SPE 118980.

Li, M., Su, K.H. & Li, Z.J. 2017. Uncertainty analysis method of casing extrusion load for ultra-deep wells. Computer Modeling in Engineering & Sciences, **113**(4): 475–495.

Goldsworthy, J. S., Jaksa, M. B. & Fenton, G. A. 2007. Effect of sample location on the reliability based design of pad foundations. Georisk, 1(3):155–166.

Maeda, Y. Yoshimi, M. & Yoshihisa, E. 2003. Stess spectrum of the jib of rough terrain crane with carrying a load. Nippon Kikai Gakkai Kotsu, Butsuryu Bumon Taikai Ronbunshu, 12: 257258-.

Yoon, J. I., Kwan, A. K. & Truong D. Q. 2009. A study on an energy saving electro-hydraulic excavator. ICCAS-SICE, 2009. IEEE: 3825–3830.

Edwards, D. J. & Holt, G. D. 2010. Case study analysis of risk from using excavators as 'cranes'. Automation in Construction, 19 (2):127133-.

Su, Y. N. & Bai, J. Z. 1991. Three dimensional analysis of down hole motor with bent sub using beam column theory. Acta Petrolei Sinica, 12(3): 110–120.

Guan, X. J. Wang, Z. D. & Liang, Y. Q. 2005. Analysis and application for the ability of drilling tools go through slim-hole horizontal well. Petroleum Drilling Techniques, 4: 26–28.

Pessier, R. C. & Fear, M. J. 1992. Quantifying common drilling problems with mechanical specific energy and a bit-specific coefficient of sliding friction. SPE 24584.

Eric, M. & Marc, H. 2004. Understanding torque: the key to slide-drilling directional wells. IADC/SPE 87162.

Long, G., Li, M. & Guan, Z. C. 2013. Evaluation method of casing safety and reliability in deep wells. Petroleum Drilling Techniques, **41**(4): 48,53.

Liu, J. T., Zhang, W. H. & Wang, Z. W. 2010. Structural reliability analysis based on number-theoretic method. Journal of Mechanical Engineering, **46**(6): 196,199.

Di, S. M. & Lomario, D. 2003. A comparison between Monte Carlo and forms in calculating the reliability of a composite structure. Composite Structures, 59:155–162 .

Blount, C. G., Hearn, D. D. & Payne, M. L. 1998. Weight on bit in coiled tubing drilling: collection and analysis of field data. SPE 46008.

Leising, L. J. Hearn, D.O. & Rike, E.A. 1996. Sidetracking technology for coiled-tubing drilling . SPE 30486.

De, S., Wen, H. & Ping Y. 2006. New approach for reliability-based design optimization . Journal of Mechanical Engineering, **19**(4):514–517.

O'Coonor, P. D. T. 2000. Commentary : reliability-past, present, and future . Ieee Transactions On Reliability, **49**(4):335–341.

Wonneberger, S. 1994. Generalization of an invertible mapping between probability and possibility . Fuzzy Sets and Systems, 64: 229–240.

Sun, Z. L. & Chen, L. Y. 2003. Practical mechanical reliability design theory and method . Beijing: Science Press.

SUBMITTED: 12/04/2018
REVISED : 08/06/2018
ACCEPTED : 04/07/2018

حساب ضغط العمل للأسطوانة الهيدروليكية لـجهاز التوجيه CTD بنـــاءً على تحليل عـــدم اليقين

منغ لي*، كان هوا سو*، لي فو وان*، جيلين ليو*، تشنغ واي تشي*، وايتشينغ تشن**

* كلية هندسة البترول جامعة تشونغتشينغ للعلوم والتكنولوجيا، تشونغتشينغ، الصين
* كلية هندسة البترول وعلوم الأرض، جامعة الملك فهد للبترول والمعادن، المملكة العربية السعودية

الخـلاصة

إن تصميم ضغط العمل للأسطوانة الهيدروليكية لجهاز التوجيه يتأثر بعشوائية الحمل (عزم الدوران) أثناء عملية الحفر الأنبوبي المستمر (CTD). وبالتالي، تم إنشاء الفكرة الأساسية لتصميم ضغط العمل للأسطوانة الهيدروليكية الخاصة بجهاز التوجيه بطريقة تحليل عدم اليقين. تم استخدام طريقة مونت كارلو لعمل اختبار إحصائي محاكي بالنسبة لبارامترات عزم الدوران وقد أثمرت عن أنماط توزيع عزم الدوران ودالات التوزيع . بناءً على نظرية الاحتمالات ووفقاً لعلاقة الدوال بين عزم الدوران وضغط العمل للأسطوانة الهيدروليكية، تم استخلاص دوال التوزيع المحتملة لضغط العمل وتحليلها باستخدام طريقة العامل الأحادي في تحليل نطاق توزيع ضغط عمل الاسطوانة الهيدروليكية. وقد أظهرت النتائج أن نظرية عدم اليقين يمكن أن تضع في عين الاعتبار وبشكل معقول في عشوائية البارامترات أثناء عملية تصميم ضغط العمل للأسطوانة الهيدروليكية في جهاز التوجيه، وخلصت إلى أن نطاق ضغط العمل للأسطوانة الهيدروليكية لم يعد منحنى أحادياً، بل يختلف وفقاً لحجم الاحتمال التراكمي. وكلما ارتفع مستوى الثقة، كلما زادت منطقة الضغط، وتقل منطقة الضغط عند وجود عكس ذلك؛ وكلما زاد الانحراف المربع المتوسط لبارامترات عزم مقاومة الاحتكاك، ازدادت منطقة الضغط، وتقل منطقة الضغط عند وجود عكس ذلك. ووفقاً لتصميم بارامترات الهندسة الفعلية، فإن نطاق ضغط العمل للأسطوانة الهيدروليكية عندما تكون موجهة CTD هو من 3.93 إلى 11.71 ميجا باسكال. إن طريقة تحليل عدم اليقين لضغط العمل تمنع بشكل فعال من الإفراط في سلامة أو عدم سلامة طرق التصميم التقليدية المحددة، وتوفر إرشادات أكثر دقة لتصميم الاسطوانات الهيدروليكية ذات الصلة.